



Lawrence Berkeley Laboratory

UNIVERSITY OF CALIFORNIA

Materials & Molecular Research Division

Submitted to Surface Science

THE INITIAL OXIDATION OF Cr(100)

A.G. Baca, L.E. Klebanoff, M.A. Schulz,
E. Paparazzo, and D.A. Shirley

July 1985

TWO-WEEK LOAN COPY

*This is a Library Circulating Copy
which may be borrowed for two weeks.*



DISCLAIMER

This document was prepared as an account of work sponsored by the United States Government. While this document is believed to contain correct information, neither the United States Government nor any agency thereof, nor the Regents of the University of California, nor any of their employees, makes any warranty, express or implied, or assumes any legal responsibility for the accuracy, completeness, or usefulness of any information, apparatus, product, or process disclosed, or represents that its use would not infringe privately owned rights. Reference herein to any specific commercial product, process, or service by its trade name, trademark, manufacturer, or otherwise, does not necessarily constitute or imply its endorsement, recommendation, or favoring by the United States Government or any agency thereof, or the Regents of the University of California. The views and opinions of authors expressed herein do not necessarily state or reflect those of the United States Government or any agency thereof or the Regents of the University of California.

The Initial Oxidation of Cr(100)

A.G. Baca,* L.E. Klebanoff,** M.A. Schulz,
E. Paparazzo,† and D.A. Shirley

Materials and Molecular Research Division
Lawrence Berkeley Laboratory
and
Department of Chemistry
University of California
Berkeley, California 94720

ABSTRACT

Electron energy loss spectroscopy (EELS), Auger spectroscopy, and low-energy electron diffraction (LEED) have been used to study oxygen chemisorption on and the initial oxidation of Cr(100). With O₂ exposures up to 5 L, Cr-O vibrational frequencies between 495-545 cm⁻¹ are observed. A Cr-O stretching frequency at 635 cm⁻¹, probably due to rhombohedral Cr₂O₃, is observed to emerge strongly by ~ 60 L. Based on a sequence of O₂ exposures at 300 K and on a second sequence with 625 K and 1175 K anneals, a model of the initial oxidation of Cr(100) is presented. Subsurface oxygen in interstitial sites with Cr atoms maintaining bulk positions is proposed to act as a nucleus for subsequent oxide growth. According to this model, oxide growth at 300 K occurs primarily through domain expansion, while frequent creation of new domains occurs at 625 K. At elevated temperatures, competition between domain growth and diffusion into the bulk is observed.

*Present address: AT&T Bell Laboratories, Murray Hill, NJ 07974.

**Present address: National Bureau of Standards, B206/220,
Gaithersburg, MD 20899.

†Permanent address: Istituto di Teoria e Struttura, Elettronica, CNR,
00016 Monterotondo, Roma, Italy.

1. INTRODUCTION

It is well known that chromium-containing surfaces form a protective oxide layer that makes them extremely stable against corrosion. It is thought that the stability of the oxide Cr_2O_3 plays a major role in this corrosion resistance, and for this reason a number of studies of the oxidation of chromium metal have been carried out. Low energy and reflection high energy electron diffraction (LEED and RHEED) [1-3] as well as scanning transmission electron microscopy micro-diffraction (STEM-MD) [4] have been used to follow the progression from two dimensional order in chemisorption to three dimensional order in Cr oxides. Auger electron spectroscopy and x-ray photoelectron spectroscopy (XPS) have been used to determine the thickness of oxide layers and to follow the kinetics of oxide growth at various temperatures [5]. Studies using work function measurements [6,7] have attempted to identify the various stages of a model of low temperature oxidation proposed by Mott and Fehlner [8]. All of the above studies observe the growth of a thin oxide layer that is common to many metals, but many details of the mechanism of the oxidation are missing, especially in the early stages. This study addresses the chemisorption and initial oxidation of Cr(100) in the temperature range 300-1175 K using LEED, Auger, and EELS.

Several workers using vibrational EELS have observed high frequency modes [9-11] that have been ascribed to subsurface sites of oxygen which are proposed to be precursors of oxidation, with metal atoms maintaining the registry of the pure metal [12]. In an

electronic EELS study of the oxidation of Cr(110), a proposed step in the oxidation can be considered consistent with the vibrational EELS model [13]. As yet there has been no detailed study of such proposed subsurface sites on any metal and their relation to subsequent oxide growth. We present a model of initial oxide domain growth and its relation to subsurface oxygen at different temperatures which lends credence to the previously proposed idea of subsurface sites as precursors to oxidation. The model sheds light on the initial transition from the chemisorbed to the oxide state that is lacking in the review of Mott and Fehlner [8].

2. EXPERIMENTAL

Our sample was a high-purity chromium single crystal that was cut and polished by standard methods. As in a previous study [14], our sample was precleaned by argon-ion bombardment (5×10^{-5} Torr, 1.5 kV) with high temperature (1120 K) cycling for three weeks to remove bulk nitrogen as detected by Auger. The crystal then displayed a very sharp, low-background (1x1) LEED pattern. No impurities were detectable by Auger, or by vibrational EELS. Oxygen adlayers were removed by brief periods of Ar ion sputtering.

Both ambient and effusive beam dosing were used for O_2 exposures. Coverages that were formed by effusive beam dosing are indicated in the data figures. When effusive beam dosing was used for O_2 exposures, approximate values of the exposures in langmuirs (L) were estimated using Auger intensities by comparison with Auger intensities of known

exposures. LEED and Auger measurements were made with LEED optics. Some samples were annealed to a given temperature for approximately five minutes using electron beam heating, and temperatures were calibrated with an infrared pyrometer.

The EEL spectrometer, based on hemispherical dispersing elements, has been described previously [15,16]. The electron monochromator is double pass, and the electron analyzer is single pass, rotatable about a solid angle of 2π . All EEL spectra were taken at 300 K, with an impact energy E_0 of 2.06 eV. Both the angle of incidence θ_i and the angle of reflection θ_r were 55° for all spectra.

3. RESULTS

Previous workers have observed some or all of the LEED pattern sequence $(1 \times 1) \rightarrow c(2 \times 2) \rightarrow (1 \times 1)$ with increasing O_2 exposure [1-3,6,17,18]. EELS measurements are reported here at coverages where these LEED patterns occur. The coverage-dependent EEL spectra of O_2 adsorption on Cr(100) at 300 K are shown in Fig. 1. After a 0.7 L exposure a very weak feature is seen at 545 cm^{-1} . This feature, as well as the absence of an intense $O=O$ stretching frequency at $\sim 800-1000 \text{ cm}^{-1}$, is indicative of dissociative chemisorption of oxygen, which is very characteristic of oxygen on transition metals in this temperature range. At this coverage, a $c(2 \times 2)$ LEED pattern, which was once thought to be characteristic of the clean surface [17], is visible. The weak intensity of the Cr-O stretch and the $O(KLL)$ Auger intensity seem to indicate that there need not be very much oxygen on the surface at a

coverage where a $c(2 \times 2)$ LEED pattern is observed. A 1.5 L O_2 exposure (not shown) gives an EEL spectrum similar in intensity and frequency to the 0.7 L exposure. As the exposure of oxygen is increased to ~ 5 L, the sticking coefficient increases, the Cr-O stretch becomes much more intense, the LEED pattern changes to (1×1) , and the mean Cr-O stretching frequency shifts to 520 cm^{-1} . The envelope becomes broad and asymmetric compared with the relatively narrow $c(2 \times 2)$ peak, and an envelope of weaker features grows in at the high energy side. As the exposure is increased further to ~ 60 L, the peak first grows broader, and then narrows considerably as a strong peak emerges at 635 cm^{-1} . At this point the Auger ratio $O(KLL)/Cr(L_{3M_{2,3}M_{4,5}})$ is nearly saturated. Diffraction studies of Cr(100) show that a thin layer of rhombohedral Cr_2O_3 forms at room temperature [1-4], which suggests assignment of the 635 cm^{-1} peak to a stretching frequency of the oxide Cr_2O_3 . All of the spectra in Fig. 1, except for the 0.7 L exposure, are inhomogeneously broadened beyond the experimental resolution of 55 cm^{-1} . The initial broadening of the spectra, followed by narrowing, suggests a high defect density associated with the initial formation of the oxide; as the oxide layer thickens, the Cr_2O_3 becomes more ordered.

The results of a second set of measurements, in which O_2 was sequentially added to the sample with thermal processing steps between exposures, are shown in Fig. 2. When Cr(100) is exposed to ~ 3 L of O_2 and the surface is heated for 5 minutes to 625 K, the spectrum shown in Fig. 2(a) is obtained. A single peak at 495 cm^{-1} is

observed, downshifted by 25–30 cm^{-1} from the region in which a room temperature peak would be expected. When the surface is then annealed to 1175 K, the spectrum in Fig. 2(b) is obtained. There are essentially no differences in the spectra other than an increase in intensity of the 495 cm^{-1} peak following the 1175 K anneal. Auger spectra show approximately the same amount of oxygen on the surface for both (a) and (b). Heat treatment alone is not sufficient to produce an oxide. A $c(2 \times 2)$ LEED pattern is also observed in each case. Addition of ~ 1 L of O_2 , followed by a brief heating of the surface to 625 K, results in the surface characterized by spectrum (c). Three additional features at 630, 755, and 960 cm^{-1} are observed in this spectrum. The 630 cm^{-1} shoulder is attributed to the oxide, but the 755 cm^{-1} and 960 cm^{-1} peaks are not observed on samples prepared and maintained at room temperature. After heating the sample to 1175 K, all features, except the 495 cm^{-1} Cr–O stretch of chemisorbed oxygen, disappear. Auger spectra show an increase of oxygen from (b) to (c) but no change in going to (d). Further addition of ~ 1 L O_2 and heating first to 625 K and then to 1175 K (Figs. 2(e) and (f)) result in spectra similar to (c) and (d). The 625 K anneal produces metastable peaks at 630, 755, and 960 cm^{-1} , which are removed by a 1175 K anneal. The LEED pattern for (c–f) reverts to (1×1) . Auger intensities were measured after each EEL spectrum in Fig. 2 and are plotted in Fig. 3. The sensitivity factors for oxygen and chromium, needed to calibrate the oxygen coverages, were determined by choosing a saturation coverage of CO dissociated on

Cr(110) as a reference compound, for which we believe there is 0.5 monolayer of oxygen [19].

The vibrational modes corresponding to the 755 cm^{-1} and 960 cm^{-1} peaks have a distinct temperature behavior. They are prominent after a 625 K anneal but not at room temperature nor after a higher temperature anneal (1175 K). In order to put forward a hypothesis to explain this, the EELS and Auger intensities will be compared for each sample (a-f) described in Fig 2. In these comparisons, it will be assumed that the EELS intensity is proportional to the number of surface oxygen atoms, though this is not strictly correct [12]. That this is not exactly correct can be seen by comparing traces (a) and (b) in Fig. 2. For different exposures at a given temperature, however, this assumption should be more reasonable, and in any case, this is the best method available for comparing oxygen in the first atomic layer to that in the first several layers. As can be seen in Fig. 4, the EELS intensity of the 495 cm^{-1} peak after the 1175 K anneals remains relatively flat above a coverage of 0.6 monolayer, while the Auger intensity (proportional to total coverage on and below the surface) increases with exposure and is nearly the same after anneals to 625 K and 1175 K. Because of the short screening length in metals, EELS is sensitive primarily to atoms above the surface, while Auger is sensitive to a depth of several atomic layers, a region which we call the "near surface" layer. The results shown in Figs. 3-4 are consistent with the interpretation that $\sim 0.6-0.7$ monolayer of oxygen is stable on the

surface at 1175 K and that any extra oxygen diffuses into the near surface layer, with ~ 10-20% diffusing into the bulk each time a 5 min. anneal at 1175 K is carried out. Presumably, longer anneals will cause even more oxygen to diffuse from the near surface layer into the bulk, but this hypothesis is not central to any of our conclusions. The data provide evidence for competition between diffusion into the bulk (favored at high temperature) and oxide nucleation and growth (favored at room temperature).

Spectra taken after 625 K anneals are the most interesting. In these spectra, the oxide (625 cm^{-1} shoulder) is less pronounced than it is at room temperature. Diffusion at 625 K should be intermediate between that at 300 K and 1175 K. Enhanced diffusion of oxygen at 625 K relative to 300 K could reduce the domain size of Cr_2O_3 . The activation energy needed for place exchange of oxygen and Cr atoms, presumably the second step (after chemisorption) in oxide formation [8,20], is more readily available at 625 K than at 300 K.

A model consistent with these ideas and with the experimental data is proposed and developed in the rest of this section. The model is illustrated qualitatively in Fig. 5. We propose that above a certain, critical coverage, oxygen migrates below the surface into sites that give a high vibrational frequency and act as precursors to the formation of oxide domains. On the timescale of our experiments these two steps may occur simultaneously. We attribute the 960 cm^{-1} and possibly also the 755 cm^{-1} peaks to oxygen in subsurface sites. According to our model, oxide growth occurs primarily through expansion and coalescence of domains as more oxygen is added at 300 K

(Fig. 5(a)). As domains coalesce, the high frequency, subsurface sites are eliminated. For thermal processing at higher temperatures (Fig. 5(b)), we propose frequent creation of new, smaller domains. Competition occurs between domain growth and diffusion of oxygen into the bulk. Figs. 5(a) and 5(b) correspond qualitatively to the sequence of exposures in Figs. 1 and 2, respectively. No particular size or shape of the domains are deduced from the data, and none are implied in Fig. 5.

The above ideas are consistent with the experimental data. If a smaller number of oxide domains are present at 300 K, then fewer precursor subsurface sites will have been formed. This is consistent with a lower intensity at 960 cm^{-1} in the 5 L exposure of Fig. 1 compared to spectra 2(c) and 2(e). The disappearance of the 960 cm^{-1} peak by $\sim 8\text{ L}$ in Fig. 1 implies some coalescence of the room temperature domains. In Fig. 2, spectra (c) and (e) are qualitatively similar yet quantitatively different in a way that supports the above model. The same thermal treatment was carried out in going from 2(b) \rightarrow 2(c) as from 2(d) \rightarrow 2(e). The only difference in the prepared surfaces is that 2(d) contains oxygen in the near surface layer and 2(b) does not. The oxygen in the near surface layer is available to form oxide when an oxide domain nucleates in 2(e) but is not available for oxide formation in 2(c). This is manifested by a greater relative intensity at 630 cm^{-1} in spectrum 2(e) compared to 2(c) and a lower intensity at 960 cm^{-1} in 2(e) vs. 2(c).

The short screening length in metals is responsible for screening

the dipole fields generated by vibrating oxygen atoms in the near surface layer and below if this layer remains metallic in character. When the near surface area is largely oxidized, as in the 60 L exposure of Fig. 1, the Cr atoms are no longer effectively screened, and the intensity of the resulting Cr-O stretch at 635 cm^{-1} increases dramatically. For spectrum 2(f), where Auger analysis shows ~ 15-20% as many oxygen as Cr atoms in the near surface layer, compared with 60-70% in the first layer, the near surface layer is largely metallic, and EELS is insensitive to oxygen below the surface. These ideas are consistent with the above model.

Although the proposed model is plausible, intuitively appealing, and self-consistent, it is also possible that bridge and atop sites are responsible for the 755 and 960 cm^{-1} peaks. The main argument against such an interpretation is as follows. It is difficult to explain why the presence of 15% oxygen in the near surface layer, a layer which remains predominantly metallic in character according to the previous discussion, should affect the populations of the bridge and atop sites. These populations are noticeably different in spectra (c) and (e) of Fig. 2. The arguments previously presented for the intensity differences in 2(c) and 2(e) are more persuasive, although the alternative possibility of bridge and atop sites cannot be ruled out.

4. DISCUSSION

Fehlner and Mott in 1970 reviewed the oxidation of metals and

proposed a model of low temperature oxidation [8] (room temperature and below) that revised the earlier ideas of Mott [21] and Cabrera and Mott [22]. Since then, much has been learned about chemisorption, adding new detail to the first stage of oxidation. Several workers have studied the transition from the chemisorption of oxygen on Cr surfaces to the oxide. Since most of these workers examine the ideas of Fehlner and Mott in relation to their own works, a brief review of the Fehlner and Mott model is given below, followed by a discussion of the implications of our results.

Room temperature oxidation begins rapidly, and the kinetics of oxygen uptake are linear. The oxidation then slows down to logarithmic kinetics and a limiting oxide thickness, usually less than 25 Å, is reached. The logarithmic growth can have a second stage in which ion transport may occur through channels, such as grain boundaries, that depend on the structure of the oxide. The mechanism for oxide growth is explained as follows: Oxygen ions formed on the surface of the thin oxide film interact with an image charge formed in the metal. This image force lowers the activation energy for a process called place exchange, in which a Cr ion changes place with an oxygen ion. If the oxide film is thin enough, the image energy may be comparable to the binding energy of a Cr atom and place exchange can occur spontaneously. Linear kinetics are then observed. If the oxide layer is thicker, a density of oxygen ions on the surface produces a voltage across the film, the Cabrera-Mott potential, which can either lower the activation barrier for continued, slower place exchange or

for oxygen transport through the oxide film, if suitable channels are present. Such channels are present in some types of amorphous, glassy oxides or at the grain boundaries of crystallites. Eventually, the oxide thickness becomes large enough that negligible lowering of the activation barrier occurs and further oxidation can take place only at elevated temperatures. The concept of place exchange is a modification of Eley and Wilkinson [20] to the earlier ideas of Cabrera and Mott [22].

Our model implies that the kinetics of place exchange in the initial nucleation of an oxide domain are different from those for place exchange occurring in an already existing domain. No attempt will be made to analyze the kinetics, but some observations can be made. Our model seems to imply that at least in the case of Cr(100) place exchange at room temperature is an activated process. If, however, place exchange on Cr(100) is an unactivated process, then at 300 K subsurface sites are populated instantaneously as soon as the surface coverage is high enough, and therefore, while O₂ is still being exposed. During the 625 K anneals, no O₂ was being exposed. Hence, if place exchange is unactivated on Cr(100), the different kinetics observed at 300 K and 625 K can be rationalized by proposing different sticking coefficients and/or different atom mobilities on parts of the surface above oxide domains at 300 K. Clearly, further experiments are needed to determine whether the model developed in this chapter is general to oxidation or specific to the sequence of experiments presented here.

If the model proposed in this paper is general, then it should be incorporated into the model of low temperature oxidation. The concept of place exchange is not challenged here, but the details of its occurrence can be made more explicit and the energetics rationalized. The energy requirements of a general place exchange mechanism are readily supplied because an oxide is thermodynamically more stable than a metal and bond energies of weakly chemisorbed atoms adsorbed at high coverages are small. In this case, the activation energy of place exchange is more important than the energetics, and, according to Fehlner and Mott [8], it is supplied by the image charge initially and by the Cabrera-Mott field at greater oxide thicknesses. However, the energetics may be different and more important for the first occurrence of place exchange, which creates a nucleus for oxide growth, than for place exchange in an existing domain. It is difficult to say what kind of an oxide can be formed initially, how many of the neighboring Cr atoms have oxide character, and if so, how much. Oxide character implies Cr-O bond lengths that are oxide-like, and for the first subsurface oxygen atom this would imply weaker metal-metal bonds which may or may not be energetically favorable overall. On the other hand, the first occurrence of place exchange to create a subsurface interstitial site is virtually guaranteed to be energetically favorable because no metal-metal bonds are broken. Furthermore, the high frequency of the precursor can be rationalized by the intact metal structure [12].

5. COMPARISON TO PREVIOUS WORK

There is general agreement from diffraction studies that rhombohedral Cr_2O_3 is formed on Cr(100) with high O_2 exposures, although there is conflict about the orientation [1-4]. The STEM-MD study proposes a spinel-like oxide which precedes the rhombohedral Cr_2O_3 . This proposal is not in conflict with the vibrational EELS data, as a great broadening in the spectra of Fig. 1 is observed before the Cr_2O_3 oxide is fully developed. The broadening could result from the initial growth of the spinel-like structure and the transition to rhombohedral Cr_2O_3 .

Allen et al. [5] studied the oxidation on Cr metal using Auger and XPS. They observed a saturation of the O(KLL) Auger signal above ~ 10 L and a gradual growth of the oxide through the core-level-shifted Cr 2p peaks at room temperature. At 600 K, thicker layers of oxide can be grown. They obtained information about the kinetics of oxide growth at various temperatures and compared this to expressions derived by Fehlner and Mott [8], but the limited resolution of XPS is not suited to uncovering the details of initial oxide growth.

Peruchetti et al. [6] studied the initial oxidation of Cr(100). They assumed that oxygen chemisorbed above the surface will produce a work function change and oxygen incorporated into the surface will not. Using these assumptions, they concluded that rapid linear oxidation occurs between 0-4 L, and that no oxygen is observed above the surface. Between 4-6 L, they concluded that oxygen adsorbs on top and that a limiting surface coverage of $\theta = 0.25$ is attained. Place

exchange was proposed to occur between 0-4 L, adsorption on the surface between 4-6 L, and continued, slow oxidation between 6-30 L. These proposals are inconsistent with the EELS data and with commonly held ideas of chemisorption. A Cr-O stretch at $\sim 520 \text{ cm}^{-1}$, characteristic of chemisorption, and a gradual transition to the oxide above $\sim 5 \text{ L}$ is observed in this work. The EELS data after 625 K and 1175 K anneals indicate that ~ 0.6 monolayer of chemisorbed oxygen above the surface is very stable.

Sakisaka et al. [13] studied the initial oxidation of Cr(110) using electronic EELS. They described the process in four steps: (1) dissociative adsorption below 2 L, (2) incorporation of oxygen below the surface between 2-6 L, (3) rapid oxidation between 6-15 L, and (4) slow thickening of the oxide film. The latter two stages are consistent with the model of Fehlner and Mott, while step (2) is consistent with the model in this paper. Steps (3) and (4) are not addressed here.

6. SUMMARY

The chemisorption and initial oxidation of Cr(100) has been studied by EELS, Auger, and LEED. Chemisorption leads to Cr-O stretching frequencies between $495\text{-}545 \text{ cm}^{-1}$. The sticking coefficient between 0-1.5 L, coverages at which a $c(2 \times 2)$ LEED pattern is observed, is lower than that between 1.5-8 L. A Cr-O stretching frequency at 635 cm^{-1} , probably due to rhombohedral Cr_2O_3 , is observed to emerge strongly by $\sim 60 \text{ L}$. Based on EELS and Auger

intensities after a sequence of O_2 exposures at 300 K and after 625 K and 1175 K anneals, a model of the initial oxidation of Cr(100) is presented. Subsurface oxygen in interstitial sites with Cr atoms maintaining bulk positions is proposed to act as a nucleus for subsequent oxide growth. According to this model, oxide growth at 300 K occurs primarily through domain expansion, while frequent creation of new domains occurs at 625 K. At elevated temperatures competition between domain growth and diffusion into the bulk is observed.

7. ACKNOWLEDGEMENTS

One of us (AGB) acknowledges a fellowship from AT&T Bell Laboratories. This work was supported by the Director, Office of Energy Research, Office of Basic Energy Sciences, Chemical Sciences Division of the U.S. Department of Energy under Contract No. DE-AC03-76SF00098.

REFERENCES

- [1] P. Michel and C. Jardin, Surf. Sci. 36 (1973) 478.
- [2] S. Ekelund and C. Leygraf, Surf. Sci. 40, (1973) 179.
- [3] H.M. Kennett and A.E. Lee, Surf. Sci. 33 (1972) 377.
- [4] F. Watari and J.M. Cowley, Surf. Sci. 105 (1981) 240.
- [5] G.C. Allen, P.M. Tucker, and R.K. Wild, JCS Faraday Trans. II, 74 (1978) 1126.
- [6] J.C. Peruchetti, G. Gewinner, and A. Jaéglé, Surf. Sci. 88 (1979) 479.
- [7] G. Gewinner, J.C. Peruchetti, A. Jaéglé, and A. Kalt, Surf. Sci. 78 (1978) 439.
- [8] F.P. Fehlner and N.F. Mott, Oxidation of Metals, 2 (1970) 59.
- [9] G. Dalmai-Imelik, J.C. Bertolini, and J. Rousseau, Surf. Sci. 63 (1977) 67.
- [10] J.L. Gland, B.A. Sexton, and G.B. Fisher, Surf. Sci. 95 (1980) 587.
- [11] W. Erley and H. Ibach, Solid State Comm. 37 (1981) 937.
- [12] H. Ibach and D.L. Mills, Electron Energy Loss Spectroscopy and Surface Vibrations, (Academic Press, New York, 1982) pp. 282-284.
- [13] Y. Sakisaka, H. Kato, and M. Onchi, Surf. Sci. 120 (1982) 150.
- [14] J.S. Foord and R.M. Lambert, Surf. Sci. 115 (1982) 141.
- [15] D.H. Rosenblatt, Ph.D. thesis, University of California, Berkeley, 1982 (LBL-14774, unpublished).
- [16] A.G. Baca, M.A. Schulz, and D.A. Shirley, J. Chem. Phys. 81 (1984) 6304.

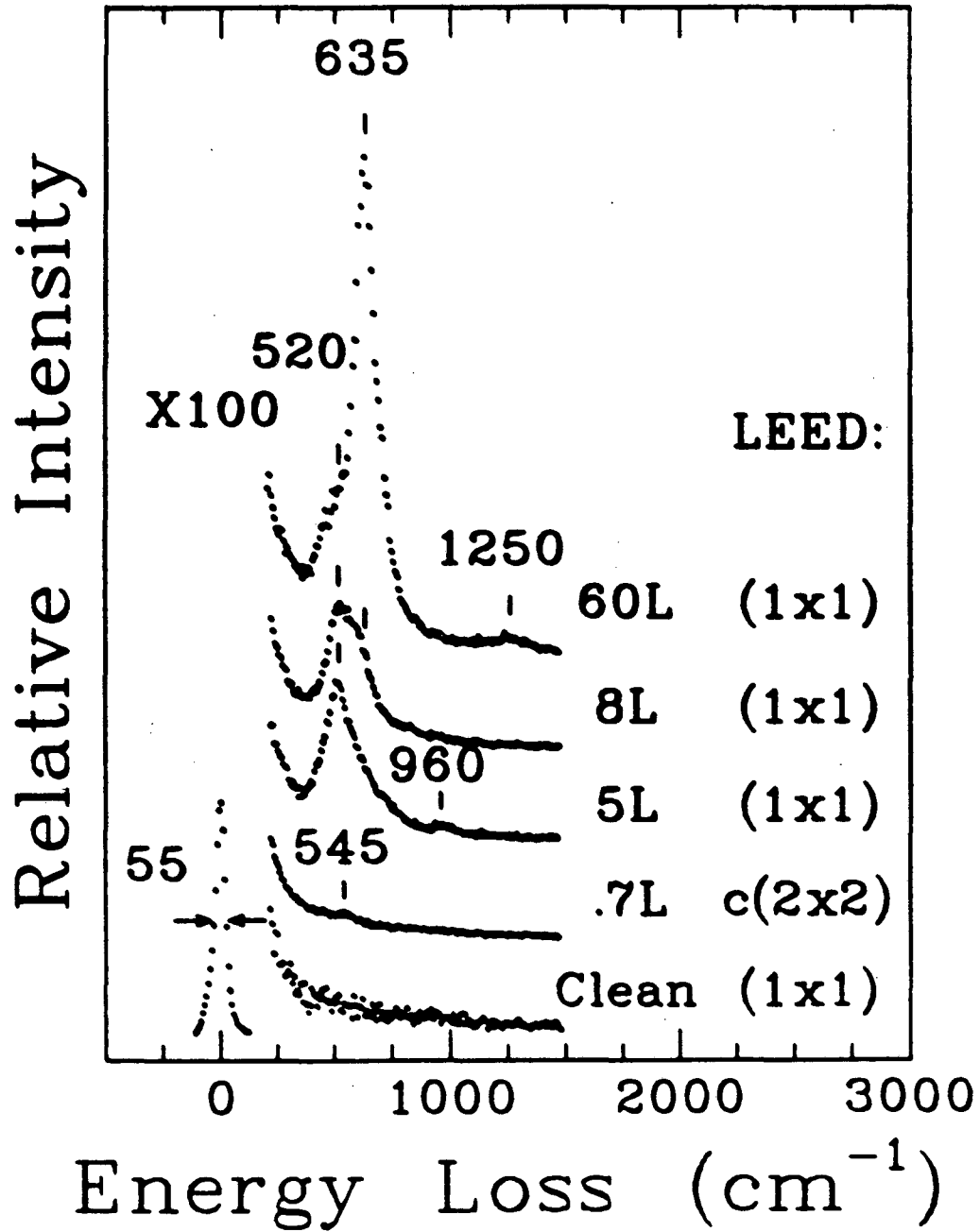
- [17] G. Gewinner, J.C. Peruchetti, A. Jaéglé, and R. Riedinger, Phys. Rev. Lett. 43 (1979) 935.
- [18] G. Gewinner, J.C. Peruchetti, and A. Jaéglé, Surf. Sci. 122 (1982) 383.
- [19] A.G. Baca, L.E. Klebanoff, M.A. Schulz, E. Papparazzo, and D.A. Shirley, submitted to Surf. Sci.
- [20] D.D. Eley and P.R. Wilkinson, Proc. Roy. Soc., Sec. A 254 (1960) 327.
- [21] N.F. Mott, Trans. Faraday Soc. 35 (1939) 1175; *ibid.* 36 (1940) 472; *ibid.* 43 (1947) 429.
- [22] N. Cabrera and N.F. Mott, Rept. Prog. Phys. 12 (1948-1949) 163.

FIGURE CAPTIONS

- Figure 1. Coverage dependence of EEL spectra for O_2 exposed to clean Cr(100) at 300 K. Exposures made in this way lead toward the oxide Cr_2O_3 . The 8 L and 60 L exposures were made with effusive beam dosing. $\theta_i = \theta_r = 55^\circ$. $E_0 = 2.06$ eV.
- Figure 2. EEL spectra for $O_2/Cr(100)$ exposures performed in the following ways: (a) A ~ 3 L exposure annealed at 625 K for 5 min., (b) annealed to 1175 K for 5 min., (c) a sequential addition of ~ 1 L at 300 K and annealed to 625 K for 5 min., (d) followed by an anneal to 1175 K for 5 min., (e) a sequential addition of ~ 1 L at 300 K and annealed to 625 K for 5 min., and (f) followed by an anneal to 1175 K for 5 min. The LEED patterns observed were $c(2 \times 2)$ for (a-b) and (1×1) for (c-f). All O_2 exposures used effusive beam dosing. $\theta_i = \theta_r = 55^\circ$. $E_0 = 2.06$ eV.
- Figure 3. Oxygen coverage vs. O_2 exposure as determined by Auger peak to peak heights in the derivative mode. A saturation coverage of CO/Cr(110) was used as a reference compound to determine the sensitivity factors of Cr and O.
- Figure 4. Intensity of the Cr-O stretch at 495 cm^{-1} vs. total coverage, including oxygen below the surface, for EEL spectra taken after 1175 K anneals.
- Figure 5. A model of the oxidation and diffusion occurring at 300 K and during the sequence of O_2 exposures described in

Fig. 2. \circ represents oxygen atoms of chemisorbed oxygen and Cr_2O_3 , and \bullet represents oxygen in the proposed subsurface sites. The solid lines represent the Cr surface, the straight dotted lines represent the boundary of the near surface layer which, of course, is not actually sharp, and the curved dotted lines represent the oxide boundary. In (a) oxidation proceeds by domain growth at 300 K, and in (b) diffusion competes with domain growth and domain creation.

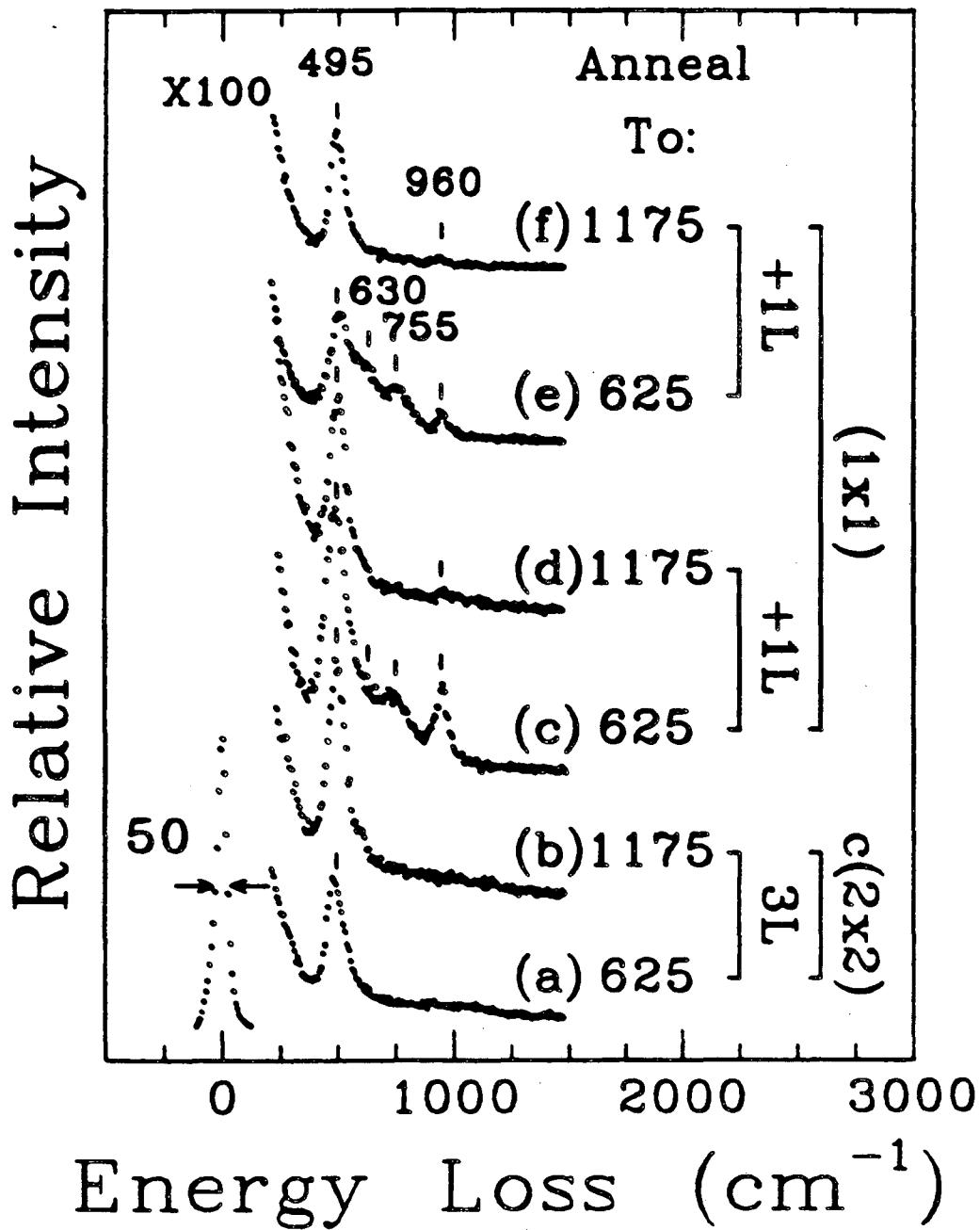
O/Cr(100) 300 K



XBL 851-776

Figure 1

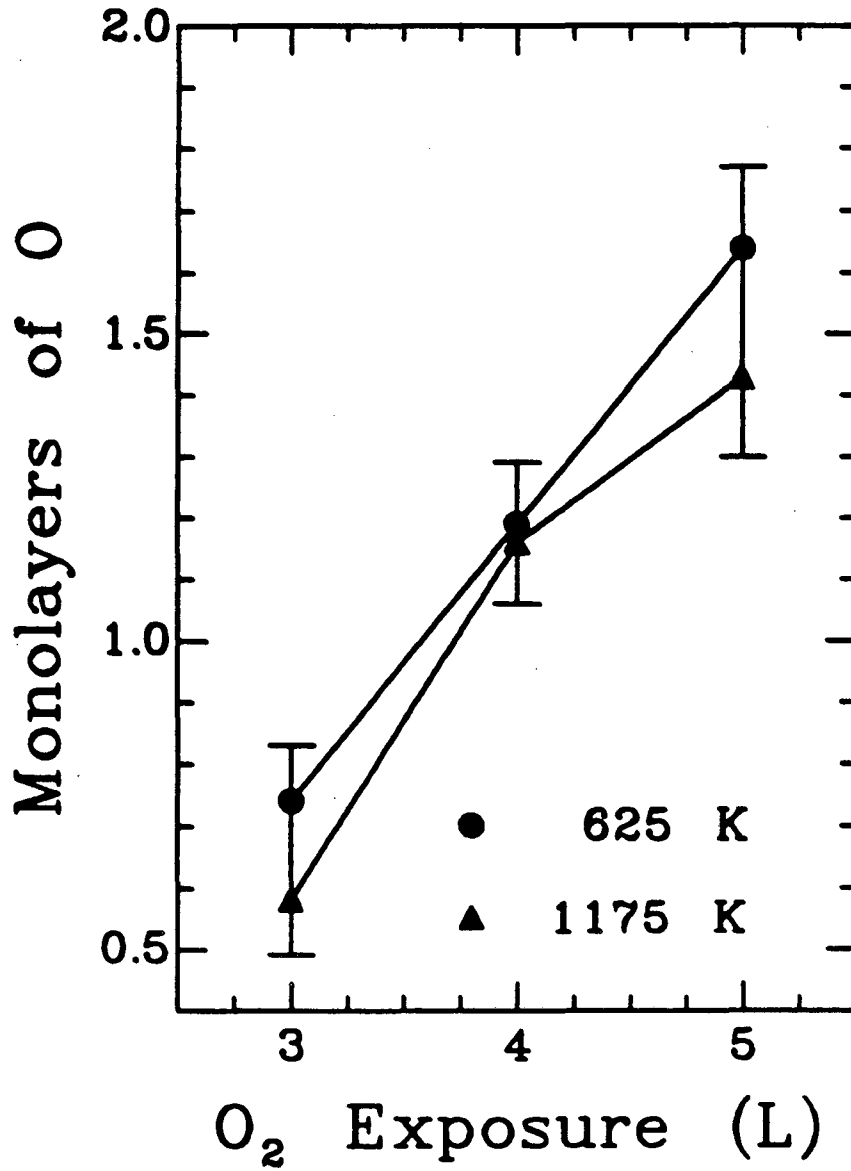
O/Cr(100)



XBL 851-778

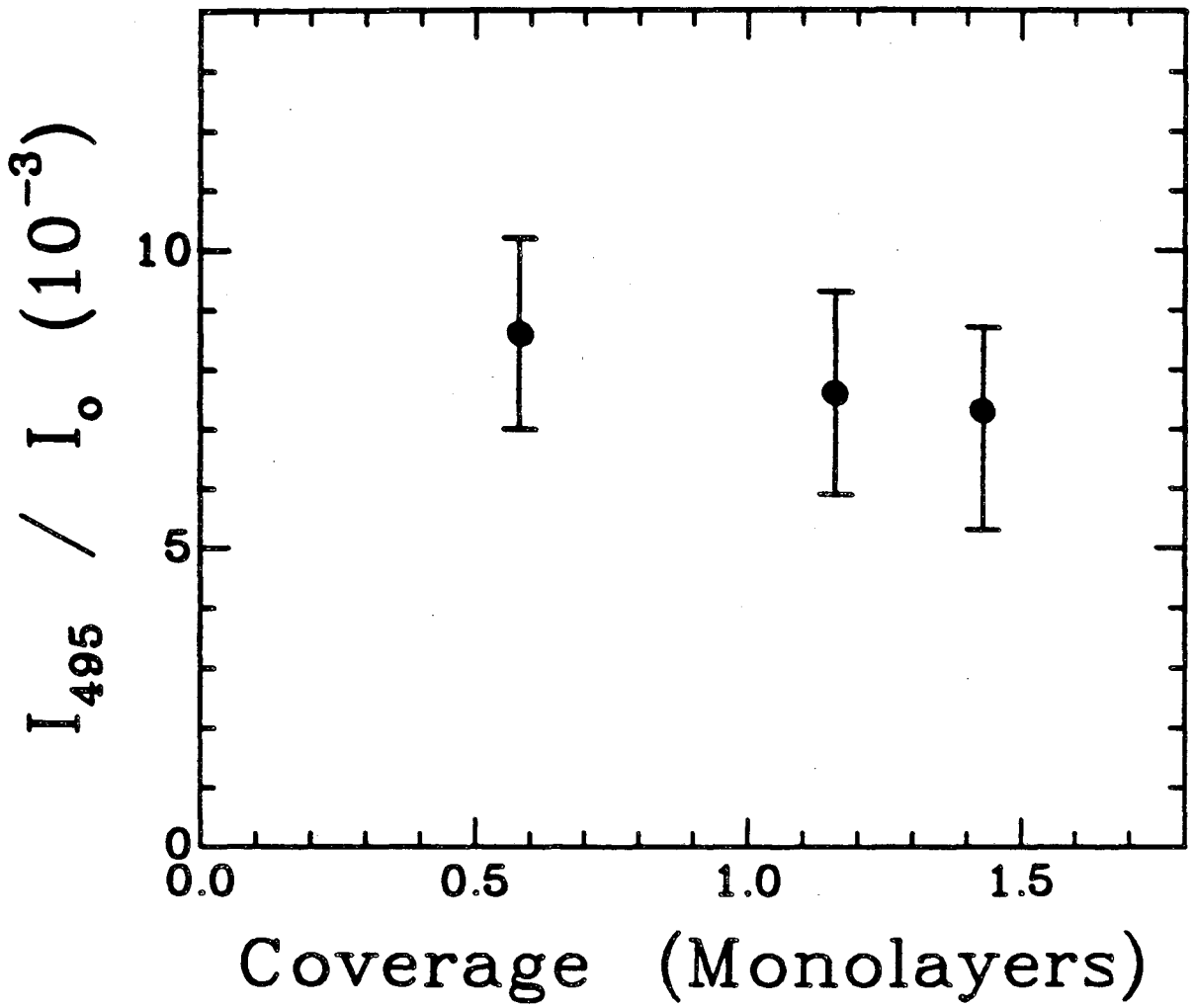
Figure 2

O/Cr(100)



XBL 851-1059

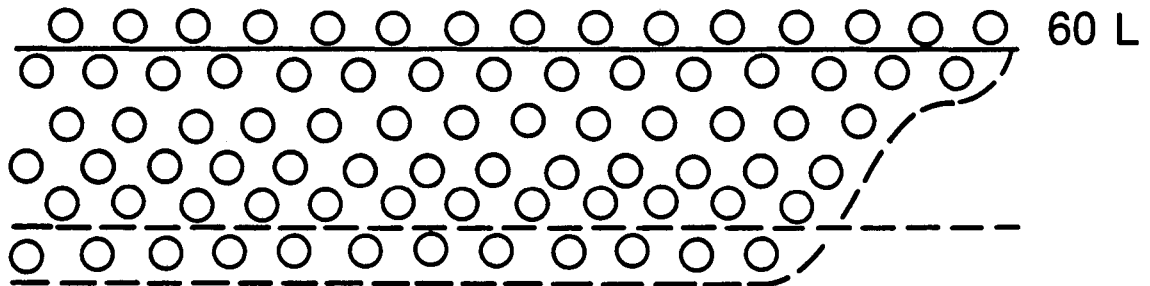
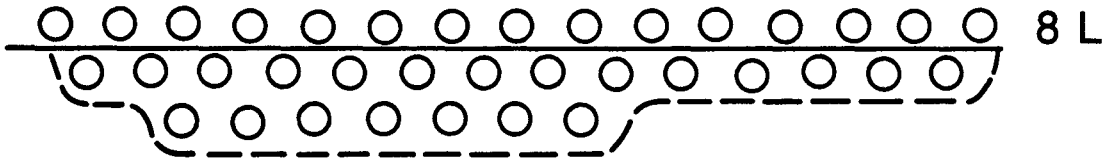
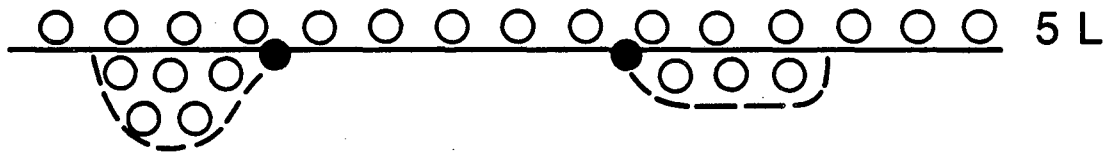
Figure 3



XBL 851-1058

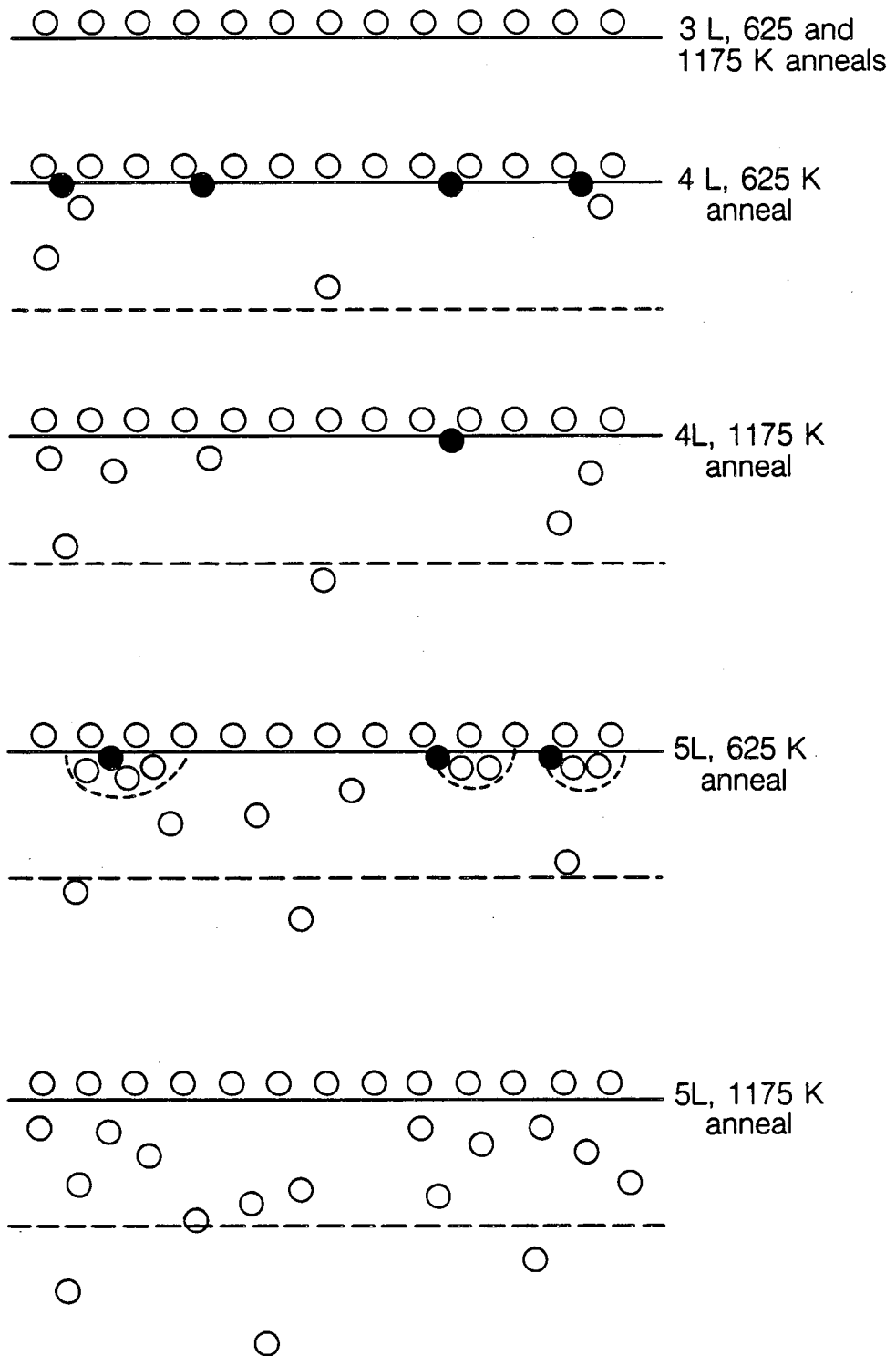
Figure 4

300 K Oxidation



XBL 851-9715

Figure 5(a)



XBL 851-772

Figure 5(b)

This report was done with support from the Department of Energy. Any conclusions or opinions expressed in this report represent solely those of the author(s) and not necessarily those of The Regents of the University of California, the Lawrence Berkeley Laboratory or the Department of Energy.

Reference to a company or product name does not imply approval or recommendation of the product by the University of California or the U.S. Department of Energy to the exclusion of others that may be suitable.

*LAWRENCE BERKELEY LABORATORY
TECHNICAL INFORMATION DEPARTMENT
UNIVERSITY OF CALIFORNIA
BERKELEY, CALIFORNIA 94720*